

## Metal–Organic Frameworks

## Fluorocarbon Separation in a Thermally Robust Zirconium Carboxylate Metal–Organic Framework

Darshika K. J. A. Wanigarathna,<sup>[a, b, c]</sup> Jiajian Gao,<sup>[c]</sup> and Bin Liu<sup>\*[a, b, c]</sup>

**Abstract:** Fluorocarbons have important applications in industry, but are environmentally unfriendly, and can cause ozone depletion and contribute to the global warming with long atmospheric lifetimes and high global warming potential. In this work, the metal–organic framework UiO-66(Zr) is demonstrated to have excellent performance characteristics to separate fluorocarbon mixtures at room temperature. Adsorption isotherm measurements of UiO-66(Zr) display high fluorocarbon sorption uptakes of 5.0 mmol g<sup>-1</sup> for R22 (CHClF<sub>2</sub>), 4.6 mmol g<sup>-1</sup> for R125 (CHF<sub>2</sub>CF<sub>3</sub>), and 2.9 mmol g<sup>-1</sup> for R32 (CH<sub>2</sub>F<sub>2</sub>) at 298 K and 1 bar. Breakthrough data obtained for binary (R22/R32 and R32/R125) and ternary (R32/R125/R134a) mixtures reveal high selectivities and capacities of UiO-66(Zr) for the separation and recycling of these fluorocarbon mixtures. Furthermore, the UiO-66(Zr) saturated with R22 and R125 can be regenerated at temperatures as low as 120 °C with excellent desorption–adsorption cycling stabilities.

With increasing concerns on ozone depletion and global warming, implementation of proper strategies to control the usage and emission of greenhouse gases has become an urgent requirement. Fluorocarbons are of great industrial importance in refrigerants, solvents, and fluoropolymers, but are environmentally unfriendly because of their long atmospheric lifetime and high ozone depletion and global warming potential.<sup>[1]</sup> Therefore, recovery, recycling and reclamation of used fluorocarbon shall greatly contribute to the prevention of

global warming and ozone depletion. The most frequently used method to recycle used fluorocarbon in large scale is cryogenic separation i.e., liquefaction followed by distillation. However, in many cases, the purity of fluorocarbons separated after distillation cannot immediately meet the industrial application standards. For example, the mixture of R32 and R125 (the boiling point of R32 and R125 are 221.3 K and 224.9 K, respectively, at atmospheric pressure) forms an azeotrope (R410A) at the composition of 50 wt.% of R32, making the complete separation of R32 from R125 extremely difficult. Furthermore, the cryogenic separation is very energy-intensive. Therefore, there is an urgent need for a commercially viable method for the separation of fluorocarbons from mixtures thereof, such that they can be reprocessed for further commercial use.


Adsorption-based separation of fluorocarbon mixtures (e.g. R22/R32/R125) is an industrially important goal, but is highly challenging because of the similar volatilities of fluorocarbon molecules with highly electronegative fluorine in the molecule, leading to similar binding interactions with the adsorbent, especially during thermodynamic selective separation. In our previous work,<sup>[2]</sup> we demonstrated the separation of R32, R22 and R125 fluorocarbon mixtures using a 4 Å molecular sieve zeolite through a molecular sieving effect. However, the low working capacity and energy-intensive regeneration process pose great challenges for large-scale industry applications. Recently, metal–organic frameworks,<sup>[3]</sup> which offer high surface area and tunable pore dimensions and pore functionality,<sup>[4]</sup> were received considerable attention for gas storage and separation,<sup>[5]</sup> including fluorocarbons.<sup>[6]</sup> Herein, we show that UiO-66(Zr), a zirconium carboxylate metal–organic framework with high degree of network connection exhibiting high fluorocarbon sorption uptakes, can be used for the separation of R22/R32, R32/R125 and R32/R125/R134a.

UiO-66(Zr),<sup>[7]</sup> a zirconium carboxylate metal–organic framework (MOF), is one of the most studied MOFs because of its excellent chemical properties and thermal stability. It consists of a cubic framework of cationic Zr<sub>6</sub>O<sub>4</sub>(OH)<sub>4</sub> nodes (formed in situ via hydrolysis of ZrCl<sub>4</sub>) connected to 12 benzene-1,4-dicarboxylate (BDC) linkers to form a 3D arrangement of micropores with each centric octahedral cage surrounded by eight corner tetrahedral cages (free diameters of ca. 11 and 8 Å for the two types of cages, respectively) and connected through narrow windows (ca. 6 Å). This framework displays a BET surface area of 1383 m<sup>2</sup> g<sup>-1</sup> and micropore volume of 0.66 cm<sup>3</sup> g<sup>-1</sup> (Figure S1 and Table S1). As compared with other common MOFs (e.g., MIL-101, MOF-5, UMCM-1, and MOF-177), the facile syn-

[a] D. K. J. A. Wanigarathna, Prof. Dr. B. Liu  
Interdisciplinary Graduate School  
Nanyang Technological University  
50 Nanyang Avenue, Singapore 639798 (Singapore)  
E-mail: liubin@ntu.edu.sg

[b] D. K. J. A. Wanigarathna, Prof. Dr. B. Liu  
Residues & Resource Reclamation Centre  
Nanyang Environment and Water Research Institute  
CleanTech One, Nanyang Technological University  
Singapore 637141 (Singapore)

[c] D. K. J. A. Wanigarathna, Dr. J. Gao, Prof. Dr. B. Liu  
School of Chemical and Biomedical Engineering  
Nanyang Technological University  
62 Nanyang Drive  
Singapore 637459 (Singapore)

 Supporting information and the ORCID identification number(s) for the author(s) of this article can be found under <https://doi.org/10.1002/asia.201800337>.

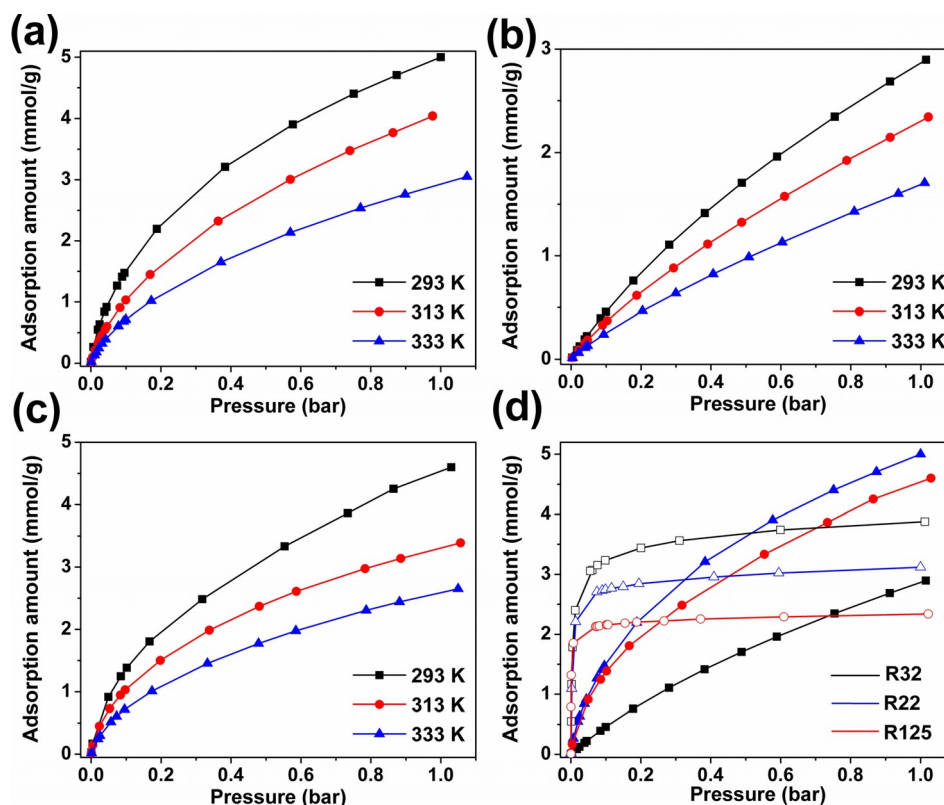


**Figure 1.** Adsorption isotherms obtained on UiO-66(Zr) for (a) R22, (b) R32, and (c) R125 at 293, 313, and 333 K, respectively and (d) comparison of adsorption isotherms at 293 K (filled and open symbols are for UiO-66(Zr) and zeolite 13X, respectively).

thesis procedure (Figure S3),<sup>[7a,8]</sup> good thermal stability together with the lack of strong-affinity binding sites could make UiO-66(Zr) a good candidate for adsorbing and desorbing fluorocarbon molecules.

To investigate the ability of UiO-66(Zr) for fluorocarbons adsorption, pure component equilibrium adsorption isotherms for R22, R32 and R125 were measured at 293, 313 and 333 K. Figure 1 displays the adsorption data. Besides, adsorption data from zeolite 13X, which is known for its high adsorption capacity, are also collected as a reference for comparison (Figure S4). As shown in Figure 1, the uptake of R22 and R125 reach 5.0 and 4.6 mmol g<sup>-1</sup>, respectively on UiO-66(Zr) at 1 bar and 293 K, which are significantly higher as compared to those on zeolite 13X (note S1 in the Supporting Information). Interestingly, although the adsorption capacity of R32 is the lowest on UiO-66(Zr), zeolite 13X exhibits the highest uptake of R32 followed by R22 and R125, which should be attributed to different adsorption mechanisms.<sup>[9]</sup>

As evidenced by the initial steep rise in the isotherms, zeolite 13X displays a strong affinity for R22, R32 and R125. On the other hand, the slow rise of the adsorption isotherms suggests moderate binding affinity of these gases on UiO-66(Zr), which is further verified by the desorption profiles that do not show any obvious hysteresis. Moderate adsorbent-adsorbate affinity is more desirable for gas separation applications as adsorbent can be more easily regenerated under milder conditions, which shall reduce the energy input required for adsorbent regeneration.

All these experimental pure gas adsorption isotherms on UiO-66(Zr) and zeolite 13X were successfully fitted with dual-site Langmuir Freundlich equation (Eq. S1) with R<sup>2</sup> value greater than 0.9999 and the obtained parameters are listed in Tables S2 and S3, respectively.

The majority of published data about MOF-based gas separation relies on many assumptions, for example, gas selectivities have often been derived from static single component adsorption isotherms instead of gas mixtures, which neglects the actual dynamic conditions. Herein, we conducted dynamic column breakthrough experiments, which can provide the insights of actual adsorption selectivities as the dynamic column breakthrough experiments closely match the real-time packed bed gas separation processes.

Figure 2a shows the breakthrough profile for the separation of R32/R125 mixture under the conditions as stated in Table S4. It is clear to see that R32 elutes from the column first followed by R125 20 minutes later, suggesting the possibility of separating near azeotropic R410A over UiO-66(Zr). The large time gap between breakthrough of R32 and R125 indicates their significant difference in sorption affinity to UiO-66(Zr). Breakthrough profile of R32 exhibits a sharp breakthrough front with a marked roll-up, suggesting that the origin of selectivity is thermodynamic.<sup>[10]</sup> At the beginning, R32 is adsorbed to a high concentration that exceeds the final equilibrium value, and then desorbs to the equilibrium as R125 penetrates. Importantly, the adsorbed R125 composition exceeds 97% while it is only 64% in the feed gas mixture. By purging the

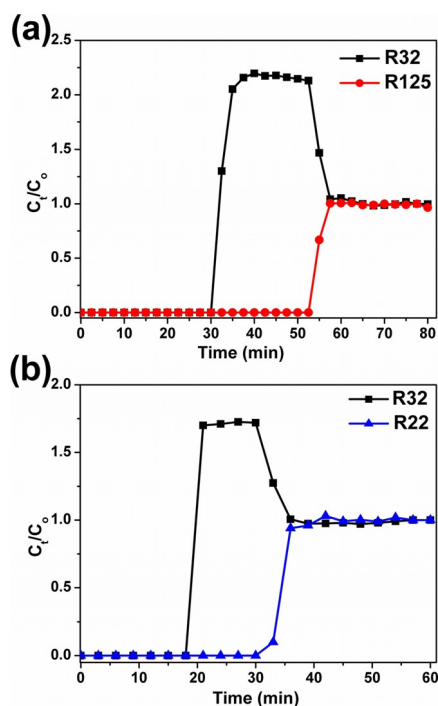


**Figure 2.** Breakthrough profiles on UiO-66(Zr) for (a) R32/R125 and (b) R32/R22 at 1 bar and 298 K.

column with pure R125 for just a few minutes, it is possible to further increase the purity of adsorbed R125. Also, it should be noted that prior to the breakthrough of R125, the gas stream leaving the column contains pure R32. Additionally, the breakthrough of R125 also displays a sharp front, indicating fast adsorption kinetics, which shall ensure complete utilization of the adsorption bed for gas separation applications.

Similar to the R32/R125 breakthrough result, R32 first leaves the adsorption column during separation of R22/R32 mixture (Figure 2b), revealing selective adsorption of R22 over R32 on UiO-66(Zr). The breakthrough profile also demonstrates the characteristic of thermodynamic separation, which displays sharp breakthrough front with marked roll-up. The composition of R22 in the adsorbed phase also reaches as high as 97%, while it is around 46% in the feed gas mixture. Therefore UiO-66(Zr) is capable to separate R22/R32 mixture as well.

In general, gases with higher polarity show stronger interaction with adsorbent,<sup>[10]</sup> which partially explains the higher selectivity of R22 and R125 over R32 on UiO-66(Zr) (polarizability varies in the sequence of R125 > R22 > R32).<sup>[11]</sup> Besides, R22 and R125 have larger molecular size and molar mass as well as higher boiling point with highly acidic H in the structure as compared to R32, which shall promote more effective van der Waals interaction and stronger C–H... $\pi$  and C–H...O interactions with the phenyl group in UiO-66(Zr), leading to selective adsorption of R22 and R125 over R32. Similarly, retaining of heavier saturated hydrocarbons (C<sub>3</sub>H<sub>8</sub>, C<sub>2</sub>H<sub>6</sub>) over light hydrocarbons (CH<sub>4</sub>) in UiO-66(Zr) has been reported in literature.<sup>[12]</sup>

For comparison, breakthrough experiments were also conducted using zeolite 13X as the adsorbent with data shown in Figure S5, which display very poor selectivity and separation

efficiency for R32/R125 and R22/32 mixtures. Since zeolite 13X has charged pore surface, it preferentially adsorbs fluorocarbon molecules with high dipole moments. Thus, contrary to the UiO-66(Zr), zeolite 13X exhibits higher adsorption capacity and selectivity towards R32 over R22 and R125.

Similar trend was also observed during our attempts to use HKUST-1 and Mg-MOF-74 metal-organic frameworks (which have coordinatively unsaturated metal sites) for the separation of R32/R125 fluorocarbon blend (Figure S6). Both adsorbents show preferential adsorption of R32 over R125, different from the UiO-66(Zr). Tentatively this adsorption behavior can be rationalized by considering the pore functionalities and physical/chemical properties of the fluorocarbons. Since the dipole moments (R32 > R125 > R22) and polarizabilities (R125 > R22 > R32) of the fluorocarbons are in the reverse order, depending on the nature of adsorption sites available for the formation of electrostatic or van der Waals interactions, the adsorption selectivity shall also be reversed. However, both HKUST-1 and Mg-MOF-74 exhibit poor adsorption selectivity as compared to UiO-66(Zr). This poor selectivity may have occurred due to suppressing of selectivity originating from the electrostatic interactions by the van der Waals interactions.

By considering change of different fluorocarbon selectivities with the change of pore functionalities, MOFs without specific strong affinity binding sites may be more suitable for the separation of R32/R125 and R32/R22 fluorocarbon blends.

The isosteric heat of adsorption ( $Q_{st}$ ) measures the average binding strength of a gas molecule on adsorbent at a specific surface coverage and is always considered for design of gas adsorption processes, which can be calculated from the Clausius–Clapeyron equation (Equation (1)) as shown below:

$$Q_{st} = R \left[ \frac{\partial \ln P}{\partial \left(\frac{1}{T}\right)} \right]_{\theta} \quad (1)$$

where  $Q_{st}$  is the isosteric heat of adsorption,  $R$  is the universal gas constant, and  $\theta$  is the fraction of the adsorbed sites at pressure  $P$  and temperature  $T$ . The calculated isosteric heat of adsorption on UiO-66(Zr) lies in the range of 18.4–17.7, 32.2–29.8 and 29.2–24.1 kJ mol<sup>-1</sup> for R32, R22, and R125 (Figure S7), respectively, which are considerably smaller as compared to those on MIL-101.<sup>[6a]</sup> The smaller heat of adsorption for R32 (18.4 kJ mol<sup>-1</sup> at loading of 0.5 mmol g<sup>-1</sup>) on UiO-66(Zr) as compared to R22 (32.2 kJ mol<sup>-1</sup>) and R125 (29.2 kJ mol<sup>-1</sup>) is consistent with the adsorption selectivity as previously discussed.

Working capacity (WC) provides a much more important consideration than absolute gas uptake to evaluate adsorbent performance in actual gas separation. We evaluated the working capacity of UiO-66(Zr) via an economically more feasible Thermal Swing Adsorption (TSA), thanks to the excellent thermal stability of UiO-66(Zr) (Figure S8). The working capacity in a TSA process is directly related to the temperature dependence of the pure gas adsorption isotherm, which can be estimated based on the difference in adsorption capacity at the adsorption and desorption temperature ( $WC = q_{ad} - q_{des}$ ).<sup>[13]</sup>

Figure 3 shows the adsorption isotherms of R22 and R125 at 293 and 393 K on UiO-66(Zr), from which, working capacities

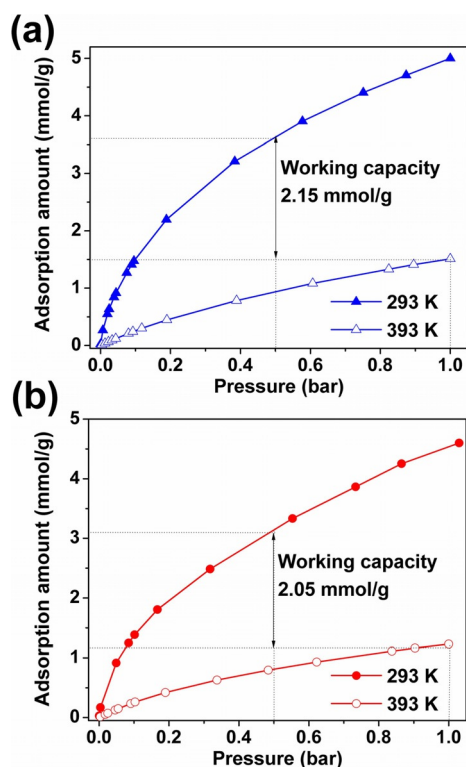


Figure 3. Estimated working capacity of (a) R22 and (b) R125 on UiO-66(Zr).

can be estimated. The adsorption amounts are obtained from pure gas adsorption isotherms at relevant loading conditions for all gases:  $q_{\text{ads}}$  at  $P_{\text{ads}}=0.5$  bar and  $T_{\text{ads}}=293$  K;  $q_{\text{des}}$  at  $P_{\text{des}}=1$  bar and  $T_{\text{des}}=393$  K. The calculated working capacity of R22 and R125 on UiO-66(Zr) are 2.15 and 2.05  $\text{mmol g}^{-1}$ , respectively, which are significantly larger than those on zeolite 13X (Figure S9).

To achieve continuous gas separation, adsorbent after reaching saturation in gas adsorption has to be regenerated. An ideal adsorbent regeneration process should minimize the energy input to remove major fraction of adsorbed gas molecules as well as should retain the adsorption performance during repeated regeneration cycles. We evaluated the regenerability (R) of UiO-66(Zr) at 393 K based on  $R(\%) = (\Delta N_1 / N_{1,\text{ads}}) \times 100$ ; where  $\Delta N_1$  is the desorbed gas amount by raising the temperature from 293 K to the desorption temperature and  $N_{1,\text{ads}}$  is the gas adsorption amount under adsorption condition at 1 bar and 293 K. Remarkably, UiO-66(Zr) exhibits very high regenerability at 393 K (reaching 70% and 73.3% for R22 and R125, respectively), while the regenerability of zeolite 13X is only 22.4% and 30.3% for R22 and R125 at the same temperature.

Besides regenerability, the cycling stability of UiO-66(Zr) was further assessed by repeatedly adsorbing and desorbing R22 and R125. Over 15 adsorption-regeneration cycles, UiO-66(Zr) exhibits stable adsorption capacity as shown in Figure 4. Figure S10 compares the XRD patterns of UiO-66(Zr) before and after 15 cycles of adsorption and regeneration operations. It is clear to see that UiO-66(Zr) well preserves its original crystal-line structure. Besides binary R32/R125 and R32/R22 mixtures, the use of UiO-66(Zr) to separate ternary R32/R125/R134a mix-

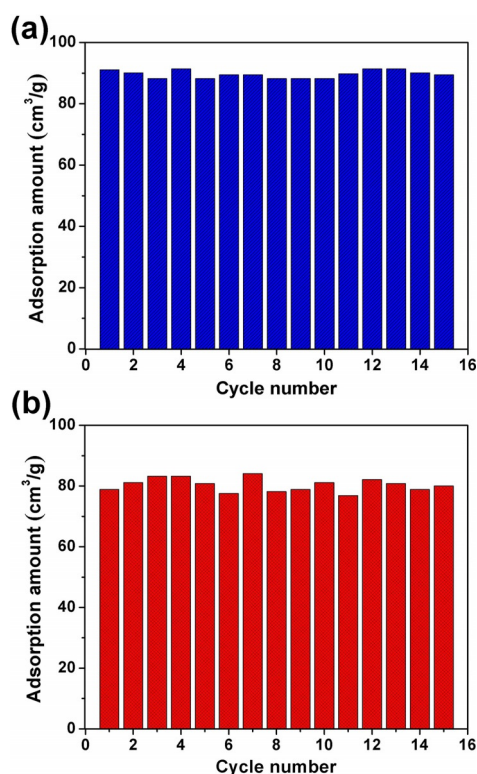


Figure 4. Cyclic R22 (a) and R125 (b) adsorption in UiO-66(Zr).

ture was also studied. Figure 5 compares the breakthrough curves of binary R32/R134a, R125/R134a and ternary R32/R125/R134a. Based on the binary breakthrough data, it is found that UiO-66(Zr) is highly suitable for separating R32/R134a with high separation efficiency, which exhibits large breakthrough time gap (Figure 5a, under the operating condition as stated in Table S4) as well as high adsorbed species purity (R134a;  $\approx 99\%$ ). Additionally, UiO-66(Zr) is also capable to separate R125/R134a blends (Figure 5b).

Therefore, it becomes possible to use UiO-66(Zr) to separate ternary R32/R125/R134a mixture. The ternary gas breakthrough curve as shown in Figure 5c exhibits different breakthrough time in the order of  $R134a > R125 > R32$ , suggesting that the adsorption strength into UiO-66(Zr) decreases in the order  $R134a > R125 > R32$ . The better selectivity of R134a on UiO-66(Zr) can be attributed to the higher boiling point of R134a (boiling point of R134a is 246.9 K, while it is 221.3 K and 224.9 K for R32 and R125, respectively), which indicates stronger gas-gas interaction and thus it is more likely to have stronger host-gas interaction as well. Besides, R134a also has higher dipole moment than R32 and R125 (dipole moments are 2.06, 1.97, 1.54 Debye for R134a, R125 and R32, respectively), which can also favorably contribute to the selective adsorption of R134a over R32 and R125.<sup>[9e]</sup>

In conclusion, we have successfully demonstrated the separation of binary R22/R32, R32/R125 and ternary R32/R125/R134a fluorocarbon mixtures in a thermally robust zirconium carboxylate metal-organic framework. The facile synthesis procedure, high adsorption capacity, outstanding selectivity, large working capacity as well as stable regeneration at low temper-

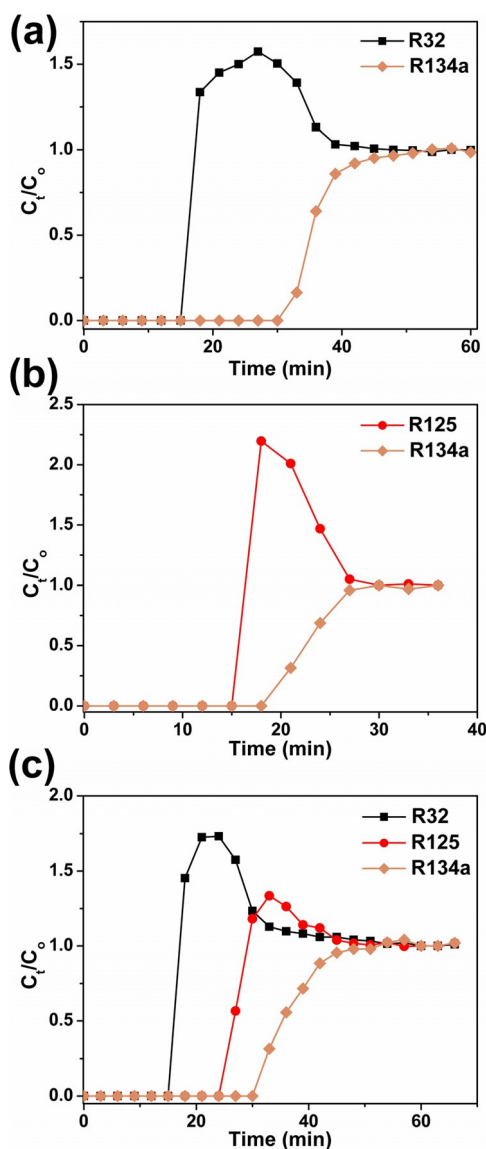


Figure 5. Breakthrough profiles on UiO-66(Zr) for (a) R32/R134a, (b) R125/R134a and (c) R32/R125/R134a at 1 bar and 298 K.

atures give the zirconium carboxylate metal–organic framework the extraordinary prospects as a solid adsorbent in the separation of fluorocarbon mixtures through temperature swing adsorption.

## Experimental Section

Details of material synthesis, characterizations, methods of obtaining pure gas adsorption isotherm measurements and breakthrough data are provided in supporting information.

## Acknowledgements

This work was supported by the Singapore National Research Foundation—Nanyang Technological University—Daioh Shinyo joint research programme.

## Conflict of interest

The authors declare no conflict of interest.

**Keywords:** adsorption • fluorocarbon • gas separation • global warming • metal–organic frameworks

- [1] Z. Zhang, Z.-Z. Yao, S. Xiang, B. Chen, *Energy Environ. Sci.* **2014**, *7*, 2868–2899.
- [2] D. J. A. Wanigarathna, J. Gao, T. Takanami, Q. Zhang, B. Liu, *ChemistrySelect* **2016**, *1*, 3718–3722.
- [3] C. A. Trickett, A. Helal, B. A. Al-Maythalyon, Z. H. Yamani, K. E. Cordova, O. M. Yaghi, *Nat. Rev. Mater.* **2017**, *2*, 17045.
- [4] a) A. M. Fracaroli, H. Furukawa, M. Suzuki, M. Dodd, S. Okajima, F. Gandara, J. A. Reimer, O. M. Yaghi, *J. Am. Chem. Soc.* **2014**, *136*, 8863–8866; b) H. Furukawa, K. E. Cordova, M. O’Keeffe, O. M. Yaghi, *Science* **2013**, *341*, 1230444–1230444; c) H. F. Rahul Banerjee, D. Britt, C. Knobler, M. O’Keeffe, O. M. Yaghi, *J. Am. Chem. Soc.* **2009**, *131*, 3875–3877.
- [5] a) J. A. Mason, K. Sumida, Z. R. Herm, R. Krishna, J. R. Long, *Energy Environ. Sci.* **2011**, *4*, 3030; b) J. A. Mason, J. Oktawiec, M. K. Taylor, M. R. Hudson, J. Rodriguez, J. E. Bachman, M. I. Gonzalez, A. Cervellino, A. Guagliardi, C. M. Brown, P. L. Llewellyn, N. Masciocchi, J. R. Long, *Nature* **2015**, *527*, 357–361.
- [6] a) R. K. Motkuri, H. V. R. Annapureddy, M. Vijaykumar, H. T. Schaefer, P. F. Martin, B. P. McGrail, L. X. Dang, R. Krishna, P. K. Thallapally, *Nat. Commun.* **2014**, *5*, 4368; b) J. Zheng, R. S. Vemuri, L. Estevez, P. K. Koech, T. Varga, D. M. Camaioni, T. A. Blake, B. P. McGrail, R. K. Motkuri, *J. Am. Chem. Soc.* **2017**, *139*, 10601–10604; c) R.-B. Lin, T.-Y. Li, H.-L. Zhou, C.-T. He, J.-P. Zhang, X.-M. Chen, *Chem. Sci.* **2015**, *6*, 2516–2521; d) C. X. Chen, S. P. Zheng, Z. W. Wei, C. C. Cao, H. P. Wang, D. Wang, J. J. Jiang, D. Fenske, C. Y. Su, *Chem. Eur. J.* **2017**, *23*, 4060–4064; e) T. H. Chen, I. Popov, W. Kavveevitthai, Y. C. Chuang, Y. S. Chen, O. Daugulis, A. J. Jacobson, O. S. Miljanic, *Nat. Commun.* **2014**, *5*, 5131; f) I. Senkovska, J. A. R. Navarro, S. Kaskel, *Microporous Mesoporous Mater.* **2012**, *156*, 115–120; g) J. Xie, F. Sun, C. Wang, Q. Pan, *Materials* **2016**, *9*, 327.
- [7] a) M. J. Katz, Z. J. Brown, Y. J. Colon, P. W. Siu, K. A. Scheidt, R. Q. Snurr, J. T. Hupp, O. K. Farha, *Chem. Commun.* **2013**, *49*, 9449–9451; b) J. H. Cavka, U. Olsbye, N. Guillou, C. Lamberti, S. Bordiga, K. P. Lillerud, *J. Am. Chem. Soc.* **2008**, *130*, 13850–13851.
- [8] a) S. Gökpinar, T. Diment, C. Janiak, *Dalton Trans.* **2017**, *46*, 9895–9900; b) M. Taddei, D. A. Steitz, J. A. van Bokhoven, M. Ranocchiari, *Chem. Eur. J.* **2016**, *22*, 3245–3249; c) Z. Hu, D. Zhao, *Dalton Trans.* **2015**, *44*, 19018–19040; d) M. Rubio-Martinez, M. P. Batten, A. Polyzos, K. C. Carey, J. I. Mardel, K. S. Lim, M. R. Hill, *Sci. Rep.* **2014**, *4*, 5443.
- [9] a) P. L. I. Daems, A. Mathivier, J. F. M. Denayer, G. V. Baron, *Stud. Surf. Sci. Catal.* **2005**, *158*, 1177–1184; b) R. Krishna, *Phys. Chem. Chem. Phys.* **2015**, *17*, 39–59; c) R. Krishna, B. Smit, S. Calero, *Chem. Soc. Rev.* **2002**, *31*, 185–194; d) J. R. Li, R. J. Kuppler, H. C. Zhou, *Chem. Soc. Rev.* **2009**, *38*, 1477–1504; e) D. K. J. A. Wanigarathna, B. Liu, J. Gao, *AIChE J.* **2018**, *64*, 640–648.
- [10] D. Peralta, G. Chaplais, A. Simon-Masseron, K. Barthelet, C. Chizallet, A. A. Quoineaud, G. D. Pirngruber, *J. Am. Chem. Soc.* **2012**, *134*, 8115–8126.
- [11] G. Morrison, *Pure Appl. Chem.* **1991**, *63*, 1465–1472.
- [12] T. Duerinck, R. Bueno-Perez, F. Vermoortele, D. E. De Vos, S. Calero, G. V. Baron, J. F. M. Denayer, *J. Phys. Chem. C* **2013**, *117*, 12567–12578.
- [13] a) W. R. Lee, H. Jo, L. M. Yang, H. Lee, D. W. Ryu, K. S. Lim, J. H. Song, D. Y. Min, S. S. Han, J. G. Seo, Y. K. Park, D. Moon, C. S. Hong, *Chem. Sci.* **2015**, *6*, 3697–3705; b) A. H. Berger, A. S. Bhowan, *Energy Procedia* **2011**, *4*, 562–567.

Manuscript received: March 2, 2018

Accepted manuscript online: March 6, 2018

Version of record online: March 22, 2018